Electroretinogram of the Cone-Dominant Thirteen-Lined Ground Squirrel during Euthermia and Hibernation in Comparison with the Rod-Dominant Brown Norway Rat

Hanmeng Zhang,[1,2] Benjamin S. Sajdak,[1–3] Dana K. Merriman,[4] Maureen A. McCall,[5] Joseph Carroll,[1,2] and Daniel M. Lipinski[1,2,6]

[1]Cell Biology, Neurobiology and Anatomy, Medical College of Wisconsin, Milwaukee, Wisconsin, United States
[2]Department of Ophthalmology and Visual Sciences, Medical College of Wisconsin, Milwaukee, Wisconsin, United States
[3]Morgridge Institute for Research, Madison, Wisconsin, United States
[4]Department of Biology, University of Wisconsin Oshkosh, Oshkosh, Wisconsin, United States
[5]Departments of Ophthalmology & Visual Sciences and Anatomical Sciences & Neurobiology, University of Louisville, Louisville, Kentucky, United States
[6]Nuffield Laboratory of Ophthalmology, University of Oxford, Oxford, United Kingdom

Correspondence: Daniel M. Lipinski, Department of Ophthalmology and Visual Sciences, 925 North 87th Street, Milwaukee, WI 53226, USA; dlipinski@mcw.edu.

Received: November 15, 2019
Accepted: April 4, 2020
Published: June 3, 2020

Citation: Zhang H, Sajdak BS, Merriman DK, McCall MA, Carroll J, Lipinski DM. Electroretinogram of the cone-dominant thirteen-lined ground squirrel during euthermia and hibernation in comparison with the rod-dominant Brown Norway rat. *Invest Ophthalmol Vis Sci.* 2020;61(6):6. https://doi.org/10.1167/iovs.61.6.6

Purpose. The majority of small animal species used in research are nocturnal, with retinae that are anatomically and functionally dissimilar from humans, complicating their use as disease models. Herein we characterize the retinal structure and electrophysiological function of the diurnal, cone-dominant 13-lined ground squirrel (13-LGS) retina during euthermia and in hibernation.

Methods. Full-field electroretinography (ERG) was performed in 13-LGS and Brown Norway (BN) rat models to establish baseline values for retinal function in each species, including following intravitreal injection of pharmacologic agents to selectively block the contributions of ON- and OFF-bipolar cells. The effect of hibernation-associated retinal remodeling on electrophysiological function was assessed in 13-LGS during torpor and emergence, with correlative histology performed using transmission electron microscopy.

Results. Under light-adapted conditions, the a-, b-, and d-wave amplitude of the 13-LGS was significantly greater than that of the BN rat. Retinal function was absent in the 13-LGS during hibernation and correlated to widespread disruption of photoreceptor and RPE structure. Remarkably, both retinal function and structure recovered rapidly on emergence from hibernation, with ERG responses reaching normal amplitude within 6 hours.

Conclusions. ERG responses for both BN rats and 13-LGS reflect the relative proportions of cone photoreceptors present within the retinae, indicating that the cone-dominant 13-LGS may be a potentially useful model for studying human central retinal function and disease. That retinal remodeling and restoration of electrophysiological function occurs rapidly on emergence from hibernation implies the 13-LGS may also be a useful tool for studying aspects of retinal physiology and recovery from injury.

Keywords: ERG, 13-lined ground squirrel, Brown Norway rat, hibernation, cone photoreceptors

In order to develop effective therapies for neurodegenerative and vascular diseases affecting the eye, it is necessary to identify and characterize animal models that accurately recapitulate specific aspects of human ocular anatomy.

Owing to their low housing and breeding costs and amenability to genetic manipulation, the most commonly utilized species in vision research remain mice (*Mus musculus*) and rats (*Rattus norvegicus*), despite them being nocturnal and having a visual system that is both structurally (e.g., no fovea) and functionally (e.g., dichromatic color vision with a small binocular field) dissimilar from humans.[1,2] By contrast, the eyes of large animal models, such as dogs, pigs, and nonhuman primates (NHPs), exhibit many anatomic and functional similarities with humans, including overlapping binocular fields, large eye size, and a defined cone-rich region in the central retina.[3–5] However, the high costs associated with acquiring and maintaining such animals, coupled with the lack of tools for rapid genetic modification and long gestation periods, severely limits their use as models of ocular disease for most laboratories.

As a small (~150 g), diurnal rodent with a highly cone-rich (~83%) retina, the 13-lined ground squirrel (13-LGS; *Ictidomys tridecemlineatus*) has been used previously to study cone-mediated vision and has been proposed as a promising model for studying diseases that affect the human central retina.[1,6–8] As an obligate hibernator whose retina

undergoes seasonal remodeling changes, the 13-LGS has additionally been identified as a potentially useful tool for studying synaptogenesis and retinal plasticity.[9]

Over the past 5 decades, numerous electrophysiological and histopathological studies have been performed on members of the squirrel family (*Sciuridae*), including the Antelope, California, European, golden-mantled, and 13-LGS, that described variously the presence of rod and cone photoreceptors with respectively slow (b2) and fast (b1) b-wave responses, the spectral sensitivities of the blue (436 nm) and green (516 nm) cone opsins, and the structural and functional recovery of the retina following retinal detachment.[10–17] More recently, our groups have also begun utilizing advanced imaging modalities, such as optical coherence tomography (OCT) and adaptive optics scanning laser ophthalmoscopy, to assess in vivo the structural changes occurring within 13-LGS retina during euthermia and hibernation.[18,19]

Although together these studies describe the basic electrophysiological and structural properties of the ground squirrel retina, the majority were conducted on animals in their nonhibernating (i.e., euthermic) state, and as a consequence do not adequately address fundamental questions as to how retinal activity is affected by hibernation, or the dynamics and extent of recovery following emergence. As these are essential considerations when proposing to use the 13-LGS as a model central retinal function or disease pathology, herein our goal was to better understand the retinal function of the 13-LGS during euthermia and hibernation. We first performed full-field electroretinography (ERG) in nonhibernating animals under dark- and light-adapted conditions to establish normative values for a-, b-, and d-wave amplitudes; for comparison, parallel ERG assessments were carried out in Brown Norway (BN) rats, which are similar in terms of body mass and eye size to the 13-LGS, but are nocturnal and possess a rod-dominant retina.[20] We subsequently probed the synaptic connectivity underlying generation of a b-wave response in both species using pharmacologic manipulations to block metabotropic (mGluR) and ionotropic (AMPA/Kainate) receptors of glutamate. Finally, we examined the light-adapted ERG responses of the 13-LGS during hibernation and throughout emergence and used transmission electron microscopy (TEM) to correlate the observed suppression of visual function with alterations in retinal ultrastructure at the outer-segments (OS) and synapse.

Methods

Animal Subjects

All experimental procedures were carried out following approval from the Institutional Animal Care and Use Committee of the Medical College of Wisconsin and were conducted in accordance with the Association for Research in Vision and Ophthalmology (ARVO) Statement for the Use of Animals in Ophthalmic and Vision Research. Ten female and eight male 13-LGSs (*I. tridecemlineatus*) aged 6 months old were obtained from the University of Wisconsin Oshkosh Squirrel Colony courtesy of Dana Merriman, PhD. Age-matched BN rats (three female, three male) were purchased from Charles River Laboratories (Wilmington, MA, USA). Among those animals, six 13-LGSs (three female, three male) and six BN rats (three female, three male) were used for standard ERG response and drug injection; twelve 13-LGSs (0 hour: 2 female, 2 male; 1 hour: 2 female; 2.5 hours: 1 female, 2 male; 6 hours: 2 female, 1 male) were used for hibernation from emergence experiment.

BN rats and euthermic 13-LGS were housed at room temperature (25°C) with food and water ad libitum under a lengthening photoperiod (12:12–14:10 light-dark) that reproduces normal seasonal changes in day length observed in southeastern Wisconsin. For hibernation studies, 13-LGSs were placed in the dark at 4°C in a hibernaculum (True Manufacturing, O'Fallon, MO, USA) without food or water. All animals in this study were utilized between November and March (2018–2019) during which time 13-LGS are at their deepest point in hibernation.[21] Once placed in hibernation, animals were left undisturbed for a period of 2 to 4 weeks to allow them to enter a cycle of "multiday torpor" interspersed with "intrabout euthermia" that typifies a normal hibernation state in this species; all assessments during hibernation were carried out during periods of multiday torpor when morphologic disruption to the retina has previously been noted by our groups.[18] Hibernating animals were monitored daily for signs of activity (e.g., cage condensation, movement of bedding). Once positioned on the ERG stage, body temperature was assessed by a FLIR E60 thermal imaging camera (FLIR Systems, Inc., Wilsonville, OR, USA).

Prior to ERG recordings, 13-LGSs (euthermic and hibernating) and BN rats were anesthetized using isoflurane (5% induction, 0.5%–4% maintenance) provided in oxygen (100%, 1 L/min). Mydriasis was induced via topical application of 2.5% phenylephrine and 1% tropicamide (Akorn, Lake Forest, IL, USA) eye drops. Topical anesthetic eye drops were not used for any procedure. An ocular speculum (Storz, Rochester, NY, USA) was used to retract the eyelids, and corneal hydration was maintained through periodic application of lubricating eye drops containing 2.5% sterile hypromellose (Akorn).

Intravitreal Injection

All intravitreal injections were performed under isoflurane anesthesia using an ophthalmic surgical microscope (Leica, Wetzlar, Germany) with bright (>1000 lux) white illumination. Following mydriasis and application of lubricating eye drops, a 6-mm circular cover slip (Fisher Scientific, Pittsburgh, PA, USA) was placed over the cornea to facilitate visualization of the neural retina under a surgical microscope. Injections were performed by partially advancing a 10-mm, 30-gauge needle trans-sclerally approximately 1 mm posterior to the limbus. The orientation and stabilization of the eye was maintained throughout the injection by manually securing the conjunctiva/sclera with notched forceps.

Following insertion of the needle, 20 µL (BN rat) or 70 µL (13-LGS) of phosphate buffered saline (PBS) containing either 2 mM 2-amino-4-phosphono-butanoic acid (known herein as L-APB) or 10 µM (*S*)-1-(2-amino-2-carboxyethyl)-3-(2-carboxy-5-phenylthiophene-3-yl-methyl)-5-methylpyrimidine-2,4-dione (known herein as ACET) was injected into the vitreous cavity over a period of 1 to 2 minutes.[22,23] The injection volumes used in this study reflect the relative differences in vitreous volumes between species and are based on prior investigator experience. Injection volumes and infusion rates were kept constant in each species regardless of the drug being administered; owing to limited animal availability, a sham injection group (e.g., PBS) was not included and so it was not possible to control for the effects of surgical intervention independently.

Investigative Ophthalmology & Visual Science

Concentrations of the pharmacologic agents were based on the literature, in which concentrations greater than 1 mM L-APB and 1 µM ACET have been shown to block the electrophysiological responses of ON- and OFF-type bipolar cells, respectively, in mice.[24,25] On completion of the injection, the needle was withdrawn and the animal transferred rapidly (within 2 minutes) to an adjacent room for light-adapted electrophysiological testing while maintaining anesthesia.

Electroretinography

Prior to manipulations, BN rats and euthermic 13-LGS were dark-adapted overnight, and all experimental setups were performed under dim red illumination. ERG recordings were carried out using an Espion E2 system (Diagnosys LLC, Cambridge, UK) with a low frequency filter of 0 Hz, high frequency filter of 1000 Hz, and notch filter of 60 Hz (Bessel filters). We were using the color dome stimulator located within a Faraday cage to minimize external electrical noise. Anesthetized BN rats and euthermic 13-LGS were positioned on a heated stage to maintain a constant body temperature of 37°C during recording. Lubricating eye drops containing 2.5% hypromellose (Akorn) were applied to the eyes to maintain corneal hydration and aid electrical conductivity. Gold wire loop electrodes were positioned on the corneal surface of both eyes, while solid core subdermal needle electrodes were inserted at the scalp and haunch to serve as reference and ground electrodes, respectively. For dark-adapted responses, brief (4 ms) single (1 Hz) white flash stimuli were delivered over a 5-log luminance series (–4 to 1 log cd.s/m^2) with the number of responses and interstimulus interval (ISI) varied with increasing luminance to reduce the effect of photobleaching (see Supplementary Table S1 for details). For dim stimuli (–4 to –3 log cd.s/m^2), 20 responses each were averaged with an ISI of 5 seconds. At –2 and –1 log cd.s/m^2, 10 responses each were averaged with an ISI of 10 seconds. At the highest luminance (0, 0.48, and 1 log cd.s/m^2), five responses each were averaged with an ISI of 20 seconds. Animals were subsequently light adapted for 10 minutes with a 25 cd/m^2 white background over which a series of brief (4 ms) single (1 Hz) flash stimuli (1, 3, and 10 log cd.s/m^2) were superimposed (20 responses each, ISI = 1 second). A long-duration (500 ms) single (1 Hz) flash stimulus (2500 cd.s/m^2, 20 responses, ISI = 1 second) and series of flicker stimuli (5, 15, and 30 Hz; 30 responses each) were also delivered under light-adapted conditions.

The 13-LGS were moved to hibernaculum in November and removed for testing in December. To perform ERGs on hibernating 13-LGS, animals were removed from the dark hibernaculum under normal room lighting conditions (500 lux) and positioned on an unheated ERG stage to prevent rapid warming during the initial (<2 minutes) light-adapted ERG recording under isoflurane anesthesia (see Supplementary Table S1). Animals were subsequently left positioned on the unheated ERG stage at room temperature (25°C) for 1, 2.5, or 6 hours to allow their body temperature to increase naturally, and at each time point ERG recordings were repeated under isoflurane anesthesia. ERG recordings at each time point were performed independently on individual animals (i.e., each animal underwent a single recording at a single time point, rather than undergoing multiple recordings). Measurements of body and eye temperature were made at the time of each ERG recording using a handheld infrared thermometer (FLIR E60, Wilsonville, OR, USA) focused either behind the ear (where there is minimal fur) or eye, respectively, from a distance of approximately 20 cm. For all the ERG data, unmasked observers used Espion E3 (Diagnosys LLC, Cambridge, UK) to manually identify waveforms (a-, b-, c- and d-waves) before values were exported into GraphPad Prism 8 (GraphPad, San Diego, CA, USA) for analysis.

For pharmacologic experiments, the long-duration (500 ms) single (1 Hz) white flash stimulus (2500 cd.s/m^2, 20 responses, ISI = 1 second) was performed immediately following injection of either L-APB or ACET and repeated every 5 minutes thereafter for a period of 30 minutes. ERG setup was performed under normal room lighting (500 lux), and recordings made with the animals positioned in a ganzfeld dome providing 25 cd/m^2 white background illumination.

Tissue Collection and Electron Microscopy (EM)

The 13-LGSs were euthanized by decapitation without recovering from anesthesia, as described previously.[26] Globes were immediately enucleated and fixed overnight at 4°C in 0.1 M cacodylate buffer containing 2% paraformaldehyde and 2% glutaraldehyde. The cornea and lens were then removed, the eye cups treated in 1% osmium buffer on ice, dehydrated using an increasing series of methanol concentrations (50%–100%), washed in acetonitrile; and embedded in 100% Epon. Embedded samples were sent to the Medical College of Wisconsin Electron Microscopy Core Facility for sectioning at a thickness of 70 nm using a PowerTome MT-XL ultramicrotome (RMC Boeckeler, Tucson, AZ, USA). Thin sections were placed on 200 mesh hexagonal grids (EMS, Hatfield, PA, USA), stained with lead citrate and uranyl acetate, and imaged with an H-600 transmission electron microscope (Hitachi High Technologies, Schaumburg, IL, USA). All images were obtained immediately inferior to the optic disc in the area of the visual streak, with eyes sectioned medially so that all samples included a portion of the horizonal optic disc, allowing us to maintain orientation.

Statistics

The D'Agostino-Pearson normality test was used to check normality of all datasets with $\alpha = 0.05$. Repeated measures 2-way ANOVA were used for comparing the differences between amplitude of 13-LGSs and BN rats ERG at different luminance or frequency stimulation with Tukey post hoc test with a 95% confidence interval ($\alpha = 0.05$). Paired *t*-tests were used for comparing the amplitudes of pre- and post-drug injection ERG recoding with a given $\alpha = 0.05$. Two-way ANOVA was used for hibernation ERG analysis with Tukey post hoc assay with a 95% confidence interval ($\alpha = 0.05$).

Results

Comparison of the Electroretinogram of Euthermic Cone-Dominant 13-LGS and Rod-Dominant BN Rats

Under dark-adapted conditions, we first performed an irradiance response series using flash stimuli of increasing luminance from –4 to 1 log cd/s.m^2. BN rat retinas were able to respond to illumination levels approximately three-orders of magnitude (–4 to –2 log cd.s/m^2) less intense than the

13-LGS, consistent with the relatively larger proportion of rod photoreceptors in the rat retina (Figs. 1A–C). At brighter flash luminance (–1 to 1 log cd.s/m^2) the a-wave amplitudes of the BN rat and 13-LGS ERG were observed to be similar, indicating that both rod and cone photoreceptors respond to bright stimuli with long ISIs under dark-adapted conditions. At the highest stimulus luminance (1 log cd.s/m^2), the b-wave amplitude of the 13-LGS ERG was significantly larger than that of the BN rat ($P < 0.0001$, repeated measures 2-way ANOVA with Tukey post hoc test, $F = 0.8257$, $DF = 1$; factor = species). Following a period of light adaptation (10 minutes), we subsequently delivered a series of single flash (1 Hz) stimuli over a range of luminance (0, 0.48, and 1 log cd.s/m^2), observing that both the a- and b-wave amplitudes were significantly greater in the 13-LGS retina than in the BN rat (Figs. 1D, 1E, 1G; repeated measures 2-way ANOVA with Tukey post hoc test; a-wave: $F = 77.98$, $DF = 1$, $P < 0.0001$ with animal model as factor; b-wave: $F = 69.14$, $DF = 1$; factor = species).

At higher luminance intensities (0.48 and 1 log cd.s/m^2) a small positive deflection immediately following the b-wave (black arrow, Fig. 1D) was observed in all 13-LGSs. To examine the hypothesis that this deflection was a d-wave response being partially obscured by the b-wave when short-duration flashes are used, we delivered a long-duration (500 ms) single flash stimulus aimed at temporally separating activation of ON- (b-wave) and OFF- (d-wave) bipolar cell responses.[27,28] A robust d-wave response was observed in the 13-LGS at light termination that was significantly greater in amplitude than that of BN rat ($P < 0.0001$, unpaired t-test), in which species the waveform is virtually absent (Figs. 1F, 1I). When using long-flash duration (500 ms) flash stimulus, the small positive deflection was instead observed on the downslope of the d-wave (Fig. 1F, black arrow) and likely represents an i-wave, a photopic response thought to originate at the level of the optic nerve that occurs at light-offset.[29]

To assess function at the RPE-photoreceptor interface in both species, we performed long-duration (5 seconds) recordings following delivery of a brief (4 ms) high luminance (10 cd.s/m^2) stimulus designed to isolate a c-wave response. Surprisingly, under both dark- and light-adapted conditions, no detectable c-wave could be recorded in the 13-LGS model, in contrast to the BN rat, in which a robust c-wave response was observed in dark-adapted animals (Supplementary Fig. S1).

Finally, we conducted a series of light-adapted (25 cd/m^2) flicker recordings at 5, 15, and 30 Hz using a bright (10 log cd.s/m^2) white stimulus to effectively isolate cone photoreceptor function from that of rods, which fail to respond to stimulus > 28 Hz, even under favorable rod-isolating conditions.[30] Although the amplitude of 13-LGS flicker responses were significantly greater than in the BN rat at all frequencies tested (Figs. 1H, 1J; repeated measures 2-way ANOVA with Tukey post hoc test, $F = 88.34$, $DF = 1$; factor = species), the amplitude of the 30-Hz response in both the 13-LGS and BN rat was significantly smaller compared with the response to slower frequency (5 and 15 Hz) stimuli, indicating that recovery kinetics appear to be slower in both models than in some other species, such as NHPs (repeated measures 2-way ANOVA with Tukey post hoc test, $F = 84.74$, $DF = 2$, $P < 0.0001$ with frequency as factor).[31]

Together these results support that vision in the 13-LGS is primarily driven by cone-photoreceptors, potentially making it a more appropriate model of human central vision than the more commonly used nocturnal rodent species.

Contribution of mGluR and Kainate Receptors to ON- and OFF-center Bipolar Cell Responses in the BN Rat and 13-LGS

To evaluate the relative contributions of ON- and OFF-type bipolar cells to the b- and d-wave responses in the 13-LGS (Figs. 1F, 1I), we performed ERG assessments pre- and postintravitreal injection of one of two pharmacologic agents, L-APB, which blocks signaling through depolarizing (ON) bipolar cells, and ACET, which blocks signaling through hyperpolarizing (OFF) bipolar cells.[24,25]

We initially performed a time course experiment to determine for each pharmacologic agent the point at which maximum ERG suppression occurred in both the 13-LGS and BN rat models ($n = 6$ per species) by delivering a long-duration flash stimulus every 5 minutes postinjection over a period of 30 minutes. We identified that L-APB and ACET administration resulted in peak ERG suppression 25- and 15-minutes postinjection, respectively, and consequently used these points for assessment in subsequent experiments (Supplementary Fig. S2).

In both the 13-LGS ($P = 0.006$) and BN rat ($P = 0.0164$, unpaired t-tests, $n = 6$ per species) a single intravitreal injection of 2 mM L-APB (mGluR agonist) effectively blocked the b-wave response (Figs. 2A–D), indicating that, consistent with other species, it is expression of mGluR6 on the dendrites of ON cone bipolar cells that mediates transmission of photoreceptor input and generation of a b-wave in the 13-LGS. L-APB administration had no significant effect on the d-wave amplitude in either species.

Injection of 10 µM ACET (Kainate receptor antagonist) resulted in a small (28.46%), but significant ($P = 0.0245$, unpaired t-test, $n = 6$) reduction in the d-wave amplitude in the 13-LGS (Figs. 2G, 2H), reflecting partial inhibition of glutamate uptake and depolarization by OFF-bipolar cells following light off-set. That the decrease in d-wave amplitude relative to preinjection baseline is only partial, however, suggests that neurotransmission between cone photoreceptor and OFF-bipolar cells may also be mediated through alternative ionotropic receptors that are not affected by ACET, or that there is crossover input from ON-bipolar cells.

Recovery of Visual Function During Emergence from Hibernation is Associated with Rapid Ultrastructural Retinal Remodeling

It has previously been noted that the retina of the 13-LGS undergoes substantial remodeling during hibernation, including shortening of the OS and synaptic ribbons.[9,18,32] To examine how these structural changes may affect retinal function, we conducted ERG assessments on 13-LGS in hibernation (denoted here as 0 hours) and at several time points during emergence (1, 2.5, and 6 hours) and harvested eyes at each time point for correlative histology by TEM. As low body temperature is known to be associated with development of cataracts in rodent species, we first performed fundoscopy and OCT to confirm that there were no significant opacities present in hibernating (0 hour) animals (Supplementary Fig. S3).[33] Fundoscopy and OCT revealed that the neural retina could be readily resolved at all stages of emergence (0, 1, 2.5, and 6 hours), indicating

Investigative Ophthalmology & Visual Science

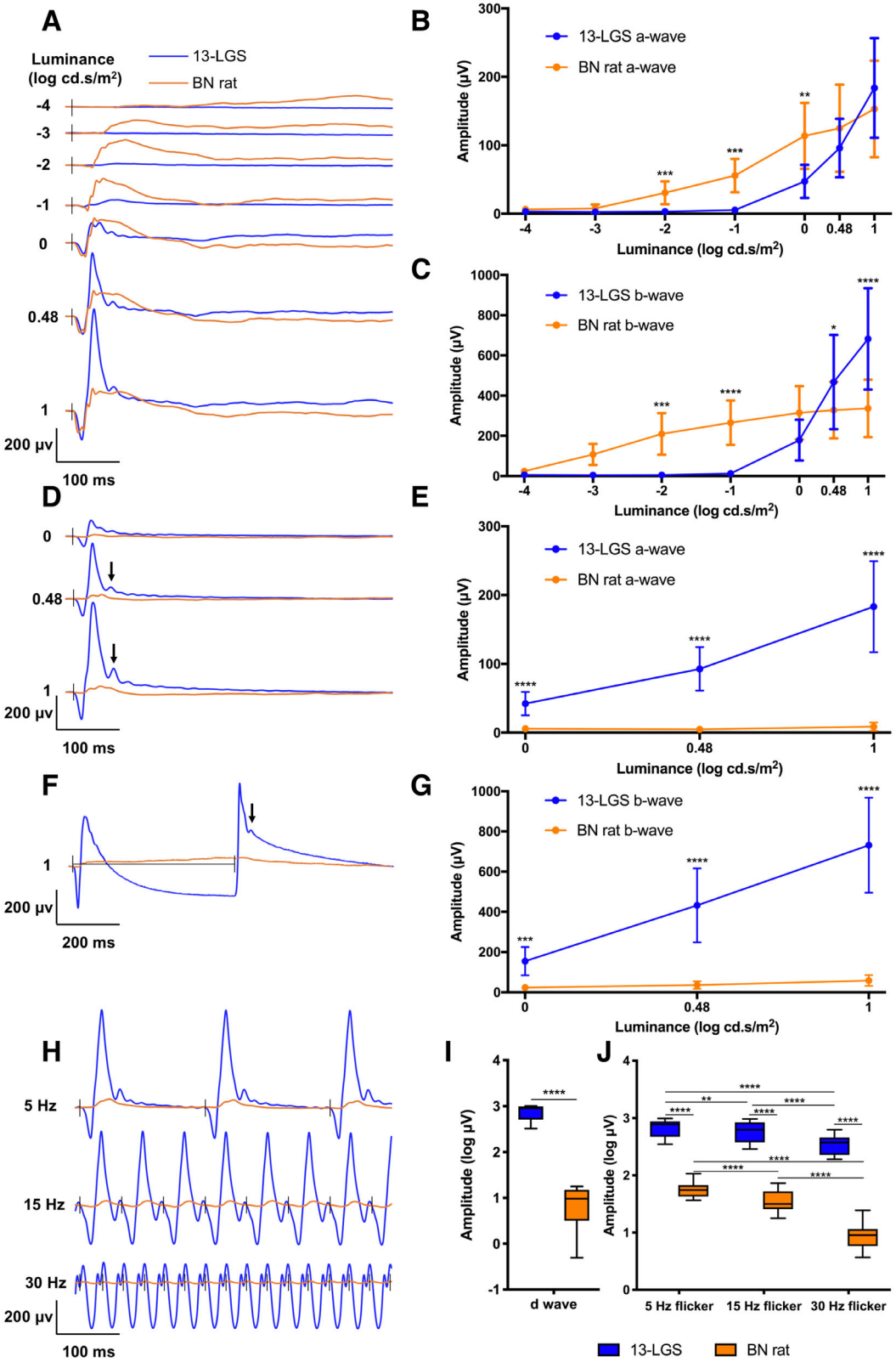

Figure 1. Comparative full-field ERG in the cone-dominant 13-LGS and rod-dominant BN rat models. Average ERG traces of 13-LGSs (n = 12, *blue*) and BN rats (n = 12, *orange*) under dark-adapted (**A**) and light-adapted (**D, F, H**) conditions following short-duration (4 ms) single flash stimuli of increasing luminance (**A, D**), a long-duration (500 ms) single flash stimulus (**F**), or a short-duration (4 ms) flicker stimulus of increasing frequency (**H**). Major wave components were subsequently quantified, including dark-adapted a- and b-waves (**B, C**), light-adapted a-, b- and d-waves (**E, G, I**), and light-adapted flicker amplitude (**J**). A small positive deflection on the down slope of the light-adapted b- and d-wave (*black arrow*) was observed only in the 13-LGS (**D, F**), which was identified as an i-wave. Repeated measures 2-way ANOVA (luminance and animal model as factors) with Sidak post hoc test were performed in all instances to allow the variance between species to be assessed independently at each luminance intensity or frequency tested. *P < 0.05; **P < 0.01; ***P < 0.001; ****P < 0.0001. Line graph error bars = SD. Box and whisker plot error bars = minimum and maximum.

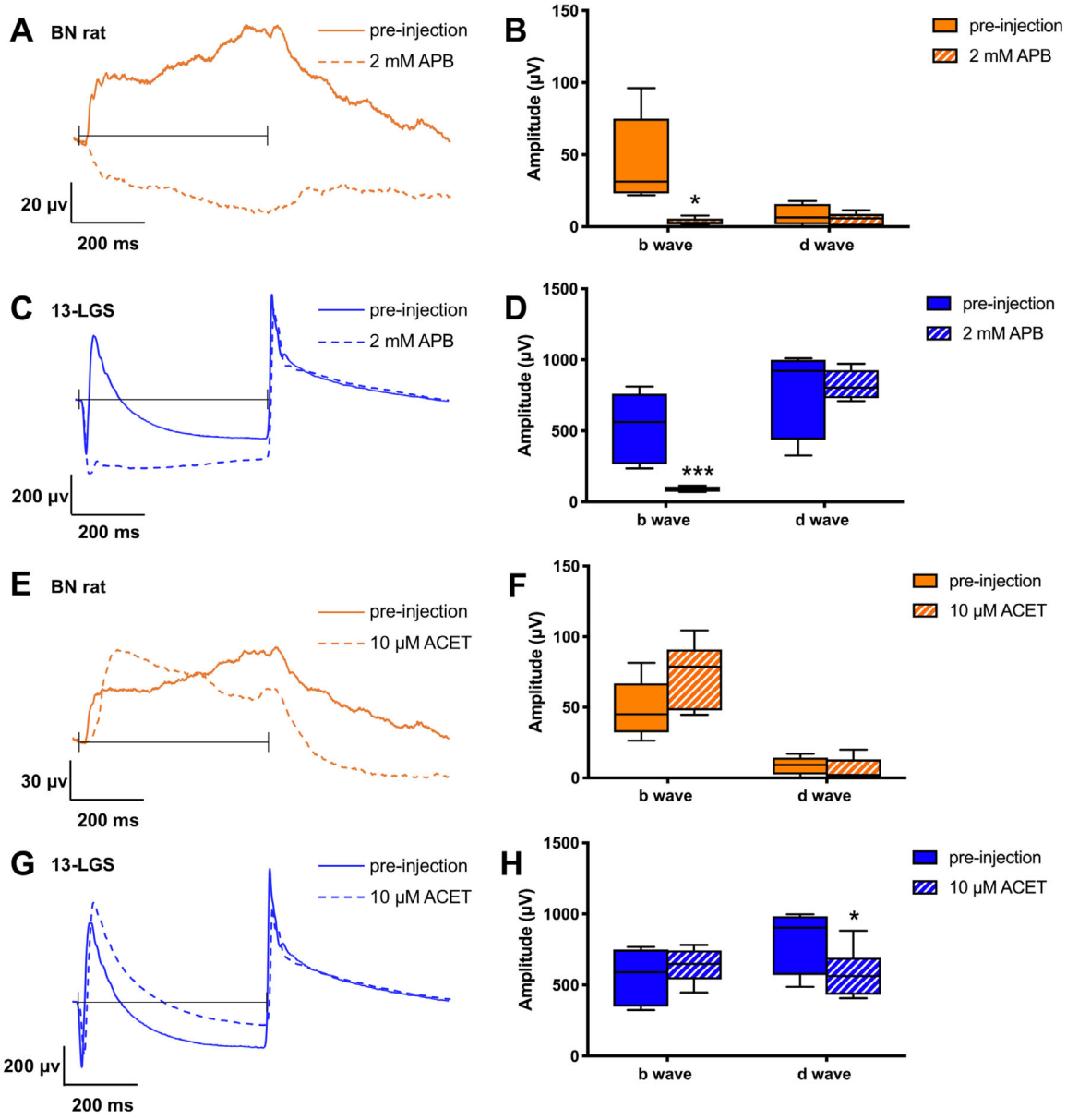

Figure 2. The effect of pharmacologic agents APB and ACET on the ERG of the 13-LGS and BN rat models. Average ERG traces of 13-LGS ($n = 6$, *blue all panels*) and BN rat ($n = 6$, *orange all panels*) pre- (*solid lines/bars*) and postintravitreal injection (*dashed lines/striped bars*) of either 2 mM APB (**A–D**) or 10 µM ACET (**E–H**) following delivery of long-duration (500 ms) single flash stimuli of fixed luminance (1 log cd.s/m^2) under light-adapted conditions. The b- and d-wave amplitude was quantified, and a series of paired *t*-tests were performed to determine effect of each drug on waveform amplitude in each species. APB injection was observed to significantly suppress b-wave amplitude in both the BN rat (**B**; $P = 0.0164$) and 13-LGS (**D**; $P = 0.006$) but did not affect amplitude of the d-wave in either species. ACET injection significantly reduced the d-wave amplitude in the 13-LGS (**H**; $P = 0.0245$), but not in the BN rat (**F**), likely due to this waveform being largely unrecordable at baseline. Box and whisker plot error bars = minimum and maximum. * = <0.05, *** = <0.001.

that any opacities present would not be of sufficient density to prevent light transmission to the retina or generation of an ERG response.

Delivery of single flash (1 Hz) stimuli over a range of luminance intensities (0, 0.48, and 1 log cd.s/m^2) in light-adapted animals revealed that cone-mediated responses were absent in the 13-LGS during hibernation (0 hour, $n = 8$) and the initial stages of emergence (1 hour, $n = 4$) (Figs. 3A, 3B, 3E), but recovered significantly in all 13-LGSs by 2.5 hours ($n = 6$; Figs. 3C, 3E; $P < 0.0001$) and reaching 101% of euthermic levels by 6 hours ($n = 6$, Figs. 3D, 3E; $P < 0.0001$; 2-way ANOVA with Tukey post hoc test, $F = 49.58$, $DF = 3$; factor = time). Although b-wave amplitudes were observed to reach euthermic levels at 6 hours postemergence, implicit times were found to be significantly slower at both 2.5 and 6 hours (when b-waves were recordable) compared with euthermic 13-LGS (Fig. 3F). Flicker ERG recordings conducted at 5, 15, and 30 Hz were also absent at 0 and 1 hour, but had recovered significantly by 6 hours postemergence (Figs. 3A–D, 3G; $P < 0.0001$ at 5, 15, and 30 Hz. Two-way ANOVA with Tukey post hoc test vs. 0 hour, $F = 108$, $DF = 3$; factor = time).

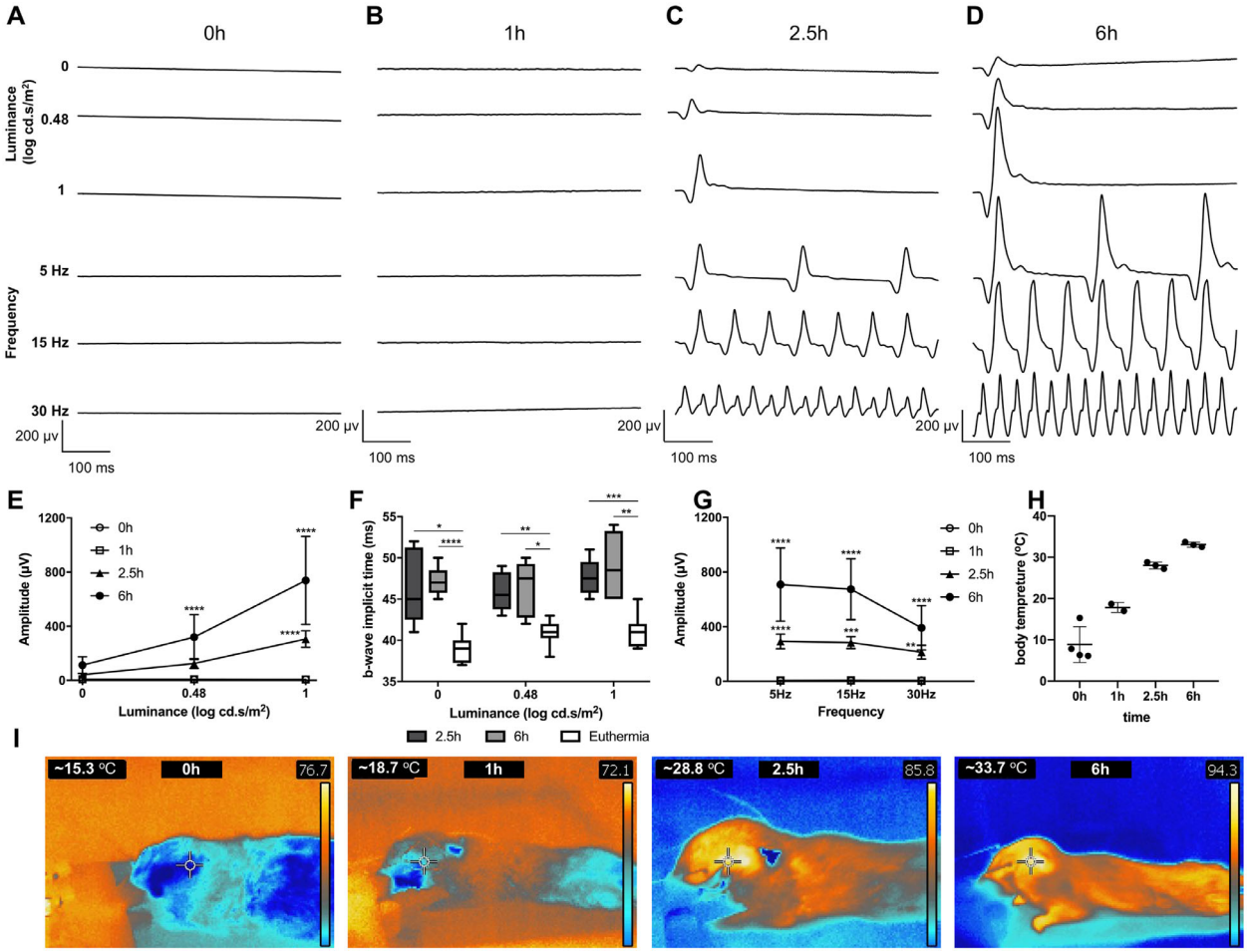

Figure 3. ERG and body temperature changes during emergence from hibernation of 13-LGSs. Average ERG traces of 13-LGS during hibernation (0 hour, $n = 8$, **A**) and at 1 hour ($n = 4$, **B**), 2.5 hours ($n = 6$, **C**), and 6 hours ($n = 6$, **D**) postemergence from hibernation following short-duration (4 ms) single flash stimuli of increasing luminance, or a short-duration (4 ms) flicker stimulus of increasing frequency. Major wave components were subsequently quantified, including light-adapted b-wave amplitude (**E**) and implicit time (**F**), and flicker amplitude (**G**) at each frequency. Repeated measures 2-way ANOVA (luminance and animal model as factors) with Tukey post hoc tests were performed in all instances to allow the variance between time points to be assessed independently at each luminance intensity or frequency tested. $^{*}P < 0.05$; $^{**}P < 0.01$; $^{***}P < 0.001$; $^{****}P < 0.0001$. Body temperature (**H**) and ocular temperature (**I**) were also assessed throughout emergence from hibernation in all animals via rectal and infrared thermometry, respectively. Line graph error bars = SD. Box and whisker plot error bars = minimum and maximum.

As body temperature is known to be a critical variable affecting ERG amplitude, we sought to correlate the observed increases in ERG amplitude to body and ocular temperature using infrared thermometry. Interestingly, although increases in body temperature (8.88°C–33.07°C; Fig. 3H) and ocular temperature (15.30°C–33.70°C; Fig. 3I) were observed over the time course (0 vs. 6 hours), normal ERG amplitudes were restored before the 13-LGS achieved a fully euthermic state (37°C), indicating that temperature increase is not the sole determinant affecting ERG recovery.[18,34]

TEM revealed that cone photoreceptors had substantially shortened OS during torpor (0 hour) and early emergence (1 hour), with misaligned or absent disks, large gaps between inner segments (IS) and OS, and rounded, loosely packed mitochondria (Figs. 4A, 4B); these findings support previous observations made by our groups using OCT that show substantial IS/OS disruption during hibernation.[18,26] In contrast to previous ultrastructural studies conducted during torpor, we also observed that the RPE appeared abnormal, lacking apical microvilli at early time points.[35] By 2.5 and 6 hours post-emergence, the outer retina had adopted a more normal morphology, wherein the photoreceptor IS possesses densely packed and elongated mitochondria, the OS contained large numbers of well-organized discs and the OS were surrounded by long apical microvilli extending from the RPE (Figs. 4C, 4D).[26]

We also used TEM to examine the synaptic connections between photoreceptors and inner retinal neurons during emergence from torpor to assess whether gross changes in neuronal connectivity were also evident. At all time points observed, cone photoreceptor pedicles appeared to be closely associated with ON- and OFF-type bipolar cells and horizontal cells of the inner retina (Figs. 4E–H), indicating that the synapses remained largely intact, even during hibernation. During torpor (0 hour) and early emergence (1 hour), however, the cone pedicle appeared abnormal with a substantially shortened ribbon synapse and a lower density of synaptic vesicles (Figs. 4E, 4F), indicating potentially decreased neurotransmitter production during torpor that

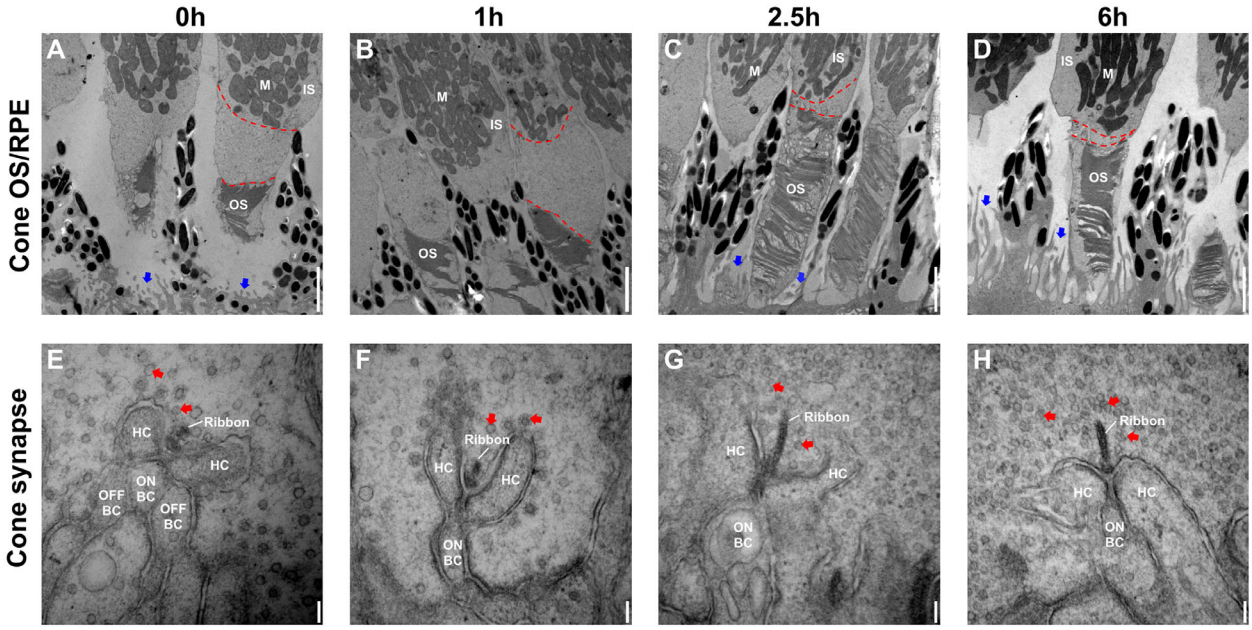

Figure 4. Transmission electron micrographs showing alterations in retinal ultrastructure in the 13-LGS during emergence from hibernation. TEM images of the IS, OS, and RPE taken from medial sections through the 13-LGS eye in the inferior retina immediately inferior to the optic disc in the area of the visual streak (**A–D**) show at early time points (0 and 1 hour) widespread disruption of OS discs, wide IS/OS junction (*red dotted line*), rounded mitochondria (M), and shortened RPE apical microvilli (*blue arrows*). TEM imaging later in emergence (2.5 and 6 hours) reveal that these structural changes have largely been reversed (**C, D**). Similarly, TEM imaging of the synaptic terminals (**E–H**) reveal a shortened ribbon synapse and relative absence of secretory vesicles (*red arrows*) at early time points (0 and 1 hour; **E, F**). As later time points (2.5 and 6 hours) the ribbon synapse has lengthened appreciably, and substantially greater numbers of synaptic vesicles are present (**G, H**). The cone pedicle was observed to remain associated to horizontal cells (HC), ON bipolar cells (ON BC) and OFF bipolar cells (OFF BC) at all time points. Lengthening of the ribbon and more synaptic vesicles apparent throughout emergence (**G, H**). (**A–D**, scale bars: 2 µm; **E–H**, scale bars: 100 nm).

may contribute to the absence of electrophysiological function.[36] At later time points (2.5 and 6 hours post-torpor), the number of synaptic vesicles present within the cone pedicle increased appreciably, and vesicles became associated with an elongated and more electron dense synaptic ribbon (Figs. 4G, 4H), indicating that the restoration of electrophysiological activity is associated with an increase in synaptic signaling, in addition to restructuring of the photoreceptor IS and OS.

Discussion

The present study represents a comprehensive comparison of retinal electrophysiological function between the nocturnal BN rat model and the diurnal 13-LGS, which owing to its small size, relatively low housing costs, and cone-dominant retina, has been proposed as a potentially useful tool for modeling human vision and ocular disease.[8,18,26,37,38] Specifically, the cone photoreceptor density and packaging geometry of the 13-LGS retina within the area of the visual streak (40,157–93,668 cells/mm) overlaps substantially with that of the human central retina in the foveal-parafoveal area (43,300–150,000 cells/mm), implying that the 13-LGS may be more useful in modelling disease affecting the central retina, such as geographic atrophy or maculopathies, than other small rodent species.[37,39]

Initially we performed parallel ERG assessments in the nocturnal BN rat and diurnal 13-LGS models under dark- and light-adapted conditions to evaluate the relative contributions of rod and cone photoreceptors to the electrophysiological response in each species, and establish normative values for major ERG components (a-, b-, c-, and d-wave) in the 13-LGS over a range of stimulus parameters. We observed that ERG responses reflected the lifestyles (nocturnal vs. diurnal) and relative proportions of rod and cone photoreceptors in the BN rat (~97% and 3%) and the 13-LGS (~17% and ~83%, respectively), with the BN rat responding better to dim intensity stimuli under dark-adapted conditions, and the 13-LGS exhibiting significantly greater ERG responses to high luminance flash and flicker stimuli in both dark- and light-adapted environments.[6,40–43]

Although the large ERG amplitudes observed in the 13-LGS can mainly be attributed to the relatively higher number and density of cone photoreceptors compared with the BN rat, a number of other anatomic factors may also contribute, including the 13-LGS having larger globe size (8.23 vs. 6.41 mm), smaller pupil diameter (3 vs. 4 mm) and longer axial length (9.45 vs. 6.29 mm).[7,37,44–46] Unfortunately, although factors such as these are known to contribute to differences in ERG response in humans, in which longer axial length and steeper corneal curvature are negatively correlated to ERG amplitude (as in myopia) and smaller pupil sizes lead to longer implicit times, for example, it is difficult to apportion the extent to which multiple (potentially) minor anatomic variations contribute to the observed ERG differences between species, even when care is taken to select an animal model with similar body and eye size for the purpose of comparison.[47,48]

In addition to there being large differences in overall amplitudes of the a- and b-waves between the 13-LGS and the BN rat, it is notable that specific other waveforms—c-wave, d-wave, and i-wave—were observed only in one

Investigative Ophthalmology & Visual Science

species in this study, indicating that there may be other fundamental differences in retinal anatomy than the 13-LGS simply having more cone photoreceptors. The 13-LGS has a large amplitude d-wave response that can be temporally separated from the b-wave using a long-duration flash stimulus, indicating that in addition to possessing significantly more cone photoreceptors than the BN rat, in which species the d-wave is largely unrecordable, the 13-LGS likely possesses a correspondingly large proportion of OFF-bipolar cells that depolarize at light off-set. Alternatively, the absence of a d-wave in rodents may reflect that specific current paths (i.e., PI) are not efficiently transmitted to (or detected at) the corneal surface as the other species, rather than there being a wholesale difference in the number or type of connecting inner retinal neurons.

Relatedly, only the 13-LGS generates a detectable i-wave, a small positive deflection that is observed on the downslope of either the b- or d-wave, depending on whether a short- (4 ms) or long-duration (500 ms) stimulus is delivered, respectively. Although the exact cellular origin of the i-wave is not fully understood—it is thought to originate at the level of the optic nerve and may derive from retinal ganglion cells—and it has been observed previously in numerous other species, including cats, rabbits, NHPs, and guinea pigs. To the authors knowledge, this is the first report of an i-wave being recorded in a member of the Sciuridae family.[29] Although the i-wave likely originates from the optic nerve, it appears only to occur in species with retinae possessing areas of high cone-density (e.g., visual streak or macular) and under photopic conditions; as such the absence of a recordable i-wave in the BN rat model in this study is entirely consistent with existing literature.[29]

More difficult to interpret is the absence of a c-wave, a slow positive deflection originating from non-neuronal cells at the RPE-photoreceptor interface, under both dark- and light-adapted conditions in the 13-LGS. It is possible that the absence of a c-wave may be the result of having relatively few rod photoreceptors within the retina, and has been noted previously in the antelope ground squirrel, raising the possibility that this is a feature shared by all diurnal members of the *Sciuridae*.[10] Considering that c-waves have been successfully recorded in other cone-dominant species (e.g., turtles), however, it may also be that the wave is present, but extremely slow, resulting in it not being detected during the recording period used in this and previous studies (3–5 seconds).[10,49] A final possibility is that because the c-wave has both an RPE and Müller cell component, the absence of a c-wave in the 13-LGS (and by extension the antelope ground squirrel) might be due to generation of a larger negative Müller cell response that counteracts the positive RPE component.[50–52]

As the 13-LGS is an obligate hibernator whose retina undergoes seasonal remodeling, we sought to correlate changes in retinal structure with electrophysiological activity during torpor and emergence. Consistent with previous studies carried out in this and other ground squirrel species, EM of the retina revealed widespread loss of photoreceptor OS disks, disorganization of the IS mitochondria, shortening of the ribbon synapse and relatively fewer synaptic vesicles during hibernation (0 hour), and early emergence (1 hour) in the 13-LGS model.[9,18,26,32,35] Importantly, by performing ERG assessments during hibernation and emergence we were able to demonstrate that the observed morphologic disruption correlated to a total absence of retinal function at any luminance tested. In contrast to previous work, we also observed substantial morphologic alterations within the RPE, with apical microvilli appearing either shortened or absent during hibernation.[32,35] Unfortunately, our attempts to assess the integrity of the RPE-photoreceptor interface directly by measuring the c-wave—a slow positive ERG waveform caused by a reduction in transepithelial potential across the RPE following light onset—were unsuccessful in the 13-LGS, even in euthermia (Supplementary Fig. S1).

Despite the extent of morphologic disruption occurring within the 13-LGS retina during hibernation, retinal function recovered extremely rapidly, with light-adapted a- and b-waves reaching normal euthermic amplitudes within 6 hours of emergence. Restoration of electrophysiological function corresponded with a period of dramatic retinal remodeling within the retina, with photoreceptors and RPE adopting a relatively normal appearance within only 6 hours of awakening, including the apparent reorganization or regrowth of OS discs, extension of apical microvilli from the RPE, reformation of the cone ribbon synapse, and increased density of synaptic vesicles. Interestingly, even though overall ERG amplitudes reverted to normal over the 6-hour time course, the implicit times of the photopic b-wave at later time points (2.5 and 6 hours) were significantly slower than that observed in nonhibernating squirrels at the same luminance intensity (Fig. 3G), indicating that the efficiency with which newly remodeled cone photoreceptors perform photoactivation and neurotransmission is initially impaired. Indeed, as several steps in the visual cycle are highly temperature dependent, including the activation, transportation, and targeting of proteins involved in phototransduction to the OS, it is highly likely that full photoreceptor functionally requires animals to achieve euthermia.[53–59] Nevertheless, that normal ERG amplitudes were achieved prior to either body or ocular temperatures reaching normal (~37°C) levels implies that restoration of some degree of visual function is an early and prioritized step on emergence from hibernation in the 13-LGS.

The reformation of the OS within such a short period is of particular interest, in which it is classically supposed that compete renewal of the cone OS takes approximately 11 to 12 days, with regrowth occurring at a rate of only 2.2 to 2.7 µm/day.[60] In injury models, the rate of regrowth has been observed to be slower still, with previous reports observing that only 40% of rod and cone OS were present 2 weeks after retinal detachment surgery was performed in NHP (*Macaca mulatta*), with complete regrowth requiring up to 5 months.[61] Even though the cone OS of 13-LGS are relatively short compared with those of other species (7–8 µm vs. up to 30 µm in humans, for example), taking an approximate rate of renewal of 2.2 to 2.7 µm/day, we believe that it is highly unlikely that cone photoreceptors in the 13-LGS are capable of de novo synthesizing a full complement of OS discs within a time frame of only 6 hours.[62]

Furthermore, the process of OS renewal is also heavily dependent on circadian rhythm and light, with turnover of rod OS happening shortly after light onset. Although cone OS renewal is more species dependent, occurring in lizards (*Sceloporus occidentalis*), chicken (*Callus domesticus*), and goldfish (*Carassius auratus L.)* at the beginning of the dark period, but happening shortly after light on-set in the cone-dominant tree shrew, all experiments in our study (including ERG and tissue harvesting for EM) were performed during daylight hours, a time when cone OS renewal would be expected to be at its slowest, regardless of species differences.[13,63–66]

Investigative Ophthalmology & Visual Science

As consequence of the limited time (6 hours) available for de novo OS synthesis and the likely effects of circadian rhythms on the rate of OS renewal during the times evaluated, we hypothesize that the apparent lack of OS discs observed with EM during torpor arises from structural disorganization, rather than actual absence. Instead, we propose that critical OS constituents (e.g., opsins) would remain present in the subretinal space rather than being degraded, thus allowing for the rapid reformation of OS discs in a circadian independent fashion and without necessitating extensive protein or lipid biosynthesis.[26] This model is supported by previous observations from our groups that cone opsins are still detectable via immunohistochemistry within the cone OS sheath even during hibernation, despite the substantial disruption to cone OS disc structure evident with TEM.[26]

Conclusions

This study provides an extensive and updated functional characterization of the 13-LGS retina during euthermia and torpor, and establishes normative values for ERG function under light- and dark-adapted conditions that could be used for reference when generating models of disease in the 13-LGS. Importantly, for the first time we also correlate normal seasonal changes in retinal ultrastructure with visual function, highlighting the rapid recovery of apparently normal vision within 6 hours of emergence from torpor. The cyclical disruption and reorganization of critical photoreceptor and RPE structures may additionally make the 13-LGS an interesting tool for studying retinal morphogenesis, neuronal plasticity, and recovery from damage.

Acknowledgments

The authors thank Lisa King, Christine Skumatz, Joseph Thulin, and the Biomedical Resource Center at the Medical College of Wisconsin for their help with animal care, in addition to Clive Wells and Robert Goodwin for their contributions to TEM sample preparation.

Supported by grants from the National Eye Institute (U24EY029891) and the Foundation for Fighting Blindness (PPA-0641-0718-UCSF and TA-NMT-0618-0739).

Disclosure: **H. Zhang,** None; **B.S. Sajdak,** None; **D.K. Merriman,** None; **M.A. McCall,** None; **J. Carroll,** None; **D.M. Lipinski,** None

References

1. Van Hooser SD, Nelson SB. The squirrel as a rodent model of the human visual system. *Vis Neurosci*. 2006;23:765–778.
2. Applebury ML, Antoch MP, Baxter LC, et al. The murine cone photoreceptor: a single cone type expresses both S and M opsins with retinal spatial patterning. *Neuron*. 2000;27:513–523.
3. Fletcher EL, Jobling AI, Vessey KA, Luu C, Guymer RH, Baird PN. Animal models of retinal disease. *Prog Mol Biol Transl Sci*. 2011;100:211–286.
4. Slijkerman RWN, Song F, Astuti GDN, et al. The pros and cons of vertebrate animal models for functional and therapeutic research on inherited retinal dystrophies. *Prog Retin Eye Res*. 2015;48:137–159.
5. Petersen-Jones SM, Komáromy AM. Dog models for blinding inherited retinal dystrophies. *Hum Gene Ther Clin Dev*. 2015;26:15–26.
6. Jacobs GH, Calderone JB, Sakai T, Lewis GP, Fisher SK. An animal model for studying cone function in retinal detachment. *Doc Ophthalmol*. 2002;104:119–132.
7. Merriman DK, Sajdak BS, Li W, Jones BW. Seasonal and post-trauma remodeling in cone-dominant ground squirrel retina. *Exp Eye Res*. 2016;150:90–105.
8. Verra DM, Sajdak BS, Merriman DK, Hicks D. Diurnal rodents as pertinent animal models of human retinal physiology and pathology. *Prog Retin Eye Res*. 2020;74:100776.
9. Mehta B, Snellman J, Chen S, Li W, Zenisek D. Synaptic ribbons influence the size and frequency of miniature-like evoked postsynaptic currents. *Neuron*. 2013;77:516–527.
10. Crescitelli F. The electroretinogram of the antelope ground squirrel. *Vision Res*. 1961;1:139–153.
11. Jacobs GH, Tootell RBH. Spectral components in thebwave of the ground squirrel electroretinogram. *Vision Res*. 1979;19:1243–1247.
12. Jacobs GH, Fisher SK, Anderson DH, Silverman MS. Scotopic and photopic vision in the California ground squirrel: physiological and anatomical evidence. *J Comp Neurol*. 1976;165:209–227.
13. Jacobs GH. Spectral sensitivity and colour vision in the ground-dwelling sciurids: results from golden mantled ground squirrels and comparisons for five species. *Anim Behav*. 1978;26:409–421.
14. Raisanen J, Dawis SM. A reweighting of receptor mechanisms in the ground squirrel retina: PIII and B-wave spectral sensitivity functions. *Brain Res*. 1983;270:311–318.
15. Jacobs GH, Neitz J. Development of spectral mechanisms in the ground squirrel retina following lid opening. *Exp Brain Res*. 1984;55:507–514.
16. Kraft TW. Photocurrents of cone photoreceptors of the golden-mantled ground squirrel. *J Physiol*. 1988;404:199–213.
17. Sakai T, Calderone JB, Lewis GP, Linberg KA, Fisher SK, Jacobs GH. Cone photoreceptor recovery after experimental detachment and reattachment: an immunocytochemical, morphological, and electrophysiological study. *Invest Ophthalmol Vis Sci*. 2003;44:416–425.
18. Sajdak BS, Salmon AE, Litts KM, et al. Evaluating seasonal changes of cone photoreceptor structure in the 13-lined ground squirrel. *Vision Res*. 2019;158:90–99.
19. Sajdak BS, Salmon AE, Linderman RE, Cava JA, Heitkotter H, Carroll J. Interocular symmetry, intraobserver repeatability, and interobserver reliability of cone density measurements in the 13-lined ground squirrel. *PLoS One*. 2019;14:e0223110.
20. Szél Á, Röhlich P. Two cone types of rat retina detected by anti-visual pigment antibodies. *Exp Eye Res*. 1992;55:47–52.
21. Williams CT, Goropashnaya AV, Buck CL, et al. Hibernating above the permafrost: effects of ambient temperature and season on expression of metabolic genes in liver and brown adipose tissue of arctic ground squirrels. *J Exp Biol*. 2011;214:1300–1306.
22. Nawy S, Jahr CE. Suppression by glutamate of cGMPactivated conductance in retinal bipolar cells. *Nature*. 1990;346:269–271.
23. Dolman NP, More JCA, Alt A, et al. Synthesis and pharmacological characterization of N3-substituted willardiine derivatives: role of the substituent at the 5-position of the uracil ring in the development of highly potent and selective GLUK5 kainate receptor antagonists. *J Med Chem*. 2007;50:1558–1570.
24. Slaughter MM, Miller RF. 2-Amino-4-phosphonobutyric acid: a new pharmacological tool for retina research. *Science*. 1981;211:182–185.

25. Puthussery T, Percival KA, Venkataramani S, Gayet-Primo J, Grünert U, Taylor WR. Kainate receptors mediate synaptic input to transient and sustained OFF visual pathways in primate retina. *J Neurosci*. 2014;34:7611–7621.
26. Sajdak BS, Bell BA, Lewis TR. et al. Assessment of outer retinal remodeling in the hibernating 13-lined ground squirrel. *Invest Opthalmol Vis Sci*. 2018;59:2538.
27. Sustar M, Holder GE, Kremers J, et al. ISCEV extended protocol for the photopic on-off ERG. *Doc Ophthalmol*. 2018;136:199–206.
28. Horn FK, Gottschalk K, Mardin CY, Pangeni G, Jünemann AG, Kremers J. On and off responses of the photopic full-field ERG in normal subjects and glaucoma patients. *Doc Ophthalmol*. 2011;122:53–62.
29. Rosolen SG, Rigaudière F, LeGargasson JF, et al. Comparing the photopic ERG i-wave in different species. *Vet Ophthalmol*. 2004;7:189–192.
30. Bush RA, Sieving PA. Inner retinal contributions to the primate photopic fast flicker electroretinogram. *J Opt Soc Am A Opt Image Sci Vis*. 1996;13:557–565.
31. Kondo M, Sieving PA. Primate photopic sine-wave flicker ERG: vector modeling analysis of component origins using glutamate analogs. *Invest Ophthalmol Vis Sci*. 2001;42:305–312.
32. Remé CE, Young RW. The effects of hibernation on cone visual cells in the ground squirrel. *Invest Ophthalmol Vis Sci*. 1977;16:815–840.
33. Benedek GB, Clark JI, Serrallach EN, et al. Light scattering and reversible cataracts in the calf and human lens. *Philos Trans R Soc A Math Phys Eng Sci*. 1979;293:329–340.
34. Carey HV, Andrews MT, Martin SL. Mammalian hibernation: cellular and molecular responses to depressed metabolism and low temperature. *Physiol Rev*. 2003;83:1153–1181.
35. Kuwabara T. Cytologic changes of the retina and pigment epithelium during hibernation. *Invest Ophthalmol*. 1975;14:457–467.
36. Li W, Chen S, Graydon C, et al. The function of the photoreceptor synaptic ribbon–a study from the hibernating ground squirrel retina. *Invest Ophthalmol Vis Sci*. 2010;51:4795–4795.
37. Sajdak B, Sulai YN, Langlo CS, et al. Noninvasive imaging of the thirteenlined ground squirrel photoreceptor mosaic. *Vis Neurosci*. 2016;33:e003.
38. Sajdak BS. Intravitreal delivery of rAA2 vectors to the 13-lined ground squirrel retina. *Invest Ophthalmol Vis Sci*. 2019;60:2896.
39. Jonas JB, Schneider U, Naumann GOH. Count and density of human retinal photoreceptors. *Graefe's Arch Clin Exp Ophthalmol*. 1992;230:505–510.
40. Kryger Z, Galli-Resta L, Jacobs GH, Reese BE. The topography of rod and cone photoreceptors in the retina of the ground squirrel. *Vis Neurosci*. 1998;15:685–691.
41. Puller C, Ondreka K, Haverkamp S. Bipolar cells of the ground squirrel retina. *J Comp Neurol*. 2011;519:759–774.
42. Mayhew TM, Astle D. Photoreceptor number and outer segment disk membrane surface area in the retina of the rat: stereological data for whole organ and average photoreceptor cell. *J Neurocytol*. 1997;26:53–61.
43. Long KO, Fisher SK. The distributions of photoreceptors and ganglion cells in the California ground squirrel, Spermophilus beecheyi. *J Comp Neurol*. 1983;221:329–340.
44. Hughes A, Wassle H. An estimate of image quality in the rat eye. *Invest Ophthalmol Vis Sci*. 1979;18:878–881.
45. Pazos M, Yang H, Gardiner SK, et al. Rat optic nerve head anatomy within 3D histomorphometric reconstructions of normal control eyes. *Exp Eye Res*. 2015;139:1–12.
46. Gur M, Sivak JG. Refractive state of the eye of a small diurnal mammal: the ground squirrel. *Am J Optom Physiol Opt*. 1979;56:689–695.
47. Sachidanandam R, Ravi P, Sen P. Effect of axial length on full-field and multifocal electroretinograms. *Clin Exp Optom*. 2017;100:668–675.
48. Westall CA, Dhaliwal HS, Panton CM, et al. Values of electroretinogram responses according to axial length. *Doc Ophthalmol*. 2001;102:115–130.
49. Matsuura T, Miller WH, Tomita T. Cone-specific c-wave in the turtle retina. *Vision Res*. 1978;18:767–775.
50. Steinberg RH, Schmidt R, Brown KT. Intracellular responses to light from cat pigment epithelium: origin of the electroretinogram c-wave. *Nature*. 1970;227:728–730.
51. Witkovsky P, Nelson J, Ripps H. Action spectra and adaptation properties of carp photoreceptors. *J Gen Physiol*. 1973;61:401–423.
52. Frishman LJ, Steinberg RH. Origin of negative potentials in the light-adapted ERG of cat retina. *J Neurophysiol*. 1990;63:1333–1346.
53. Baylor DA, Matthews G, Yau KW. Two components of electrical dark noise in toad retinal rod outer segments. *J Physiol*. 1980;309:591–621.
54. Sampath AP, Baylor DA. Molecular mechanism of spontaneous pigment activation in retinal cones. *Biophys J*. 2002;83:184–193.
55. Luo DG, Xue T, Yau KW. How vision begins: an odyssey. *Proc Natl Acad Sci USA*. 2008;105:9855–9862.
56. Ala-Laurila P, Donner K, Crouch RK, Cornwall MC. Chromophore switch from 11-cis-dehydroretinal (A2) to 11-cisretinal (A1) decreases dark noise in salamander red rods. *J Physiol*. 2007;585:57–74.
57. Ohba T, Schirmer EC, Nishimoto T, Gerace L. Energy- and temperature-dependent transport of integral proteins to the inner nuclear membrane via the nuclear pore. *J Cell Biol*. 2004;167:1051–1062.
58. Saraste J, Palade GE, Farquhar MG. Temperature-sensitive steps in the transport of secretory proteins through the Golgi complex in exocrine pancreatic cells. *Proc Natl Acad Sci USA*. 1986;83:6425–6429.
59. Matsumoto B, Besharse JC. Light and temperature modulated staining of the rod outer segment distal tips with Lucifer yellow. *Invest Ophthalmol Vis Sci*. 1985;26:628–635.
60. Jonnal RS, Besecker JR, Derby JC, et al. Imaging outer segment renewal in living human cone photoreceptors. *Opt Express*. 2010;18: 5257.
61. Guérin CJ, Lewis GP, Fisher SK, Anderson DH. Recovery of photoreceptor outer segment length and analysis of membrane assembly rates in regenerating primate photoreceptor outer segments. *Invest Ophthalmol Vis Sci*. 1993;34:175–183.
62. Anderson DH, Fisher SK, Steinberg RH. Mammalian cones: disc shedding, phagocytosis, and renewal. *Invest Ophthalmol Vis Sci*. 1978;17:117–133.
63. Bobu C, Hicks D. Regulation of retinal photoreceptor phagocytosis in a diurnal mammal by circadian clocks and ambient lighting. *Invest Opthalmol Vis Sci*. 2009;50: 3495.
64. Young RW. The daily rhythm of shedding and degradation of rod and cone outer segment membranes in the chick retina. *Invest Ophthalmol Vis Sci*. 1978;17:105–116.
65. O'Day WT, Young RW. Rhythmic daily shedding of outersegment membranes by visual cells in the goldfish. *J Cell Biol*. 1978;76:593–604.
66. Immel JH, Fisher SK. Cone photoreceptor shedding in the tree shrew (Tupaia belangerii). *Cell Tissue Res*. 1985;239:667–675.

Investigative Ophthalmology & Visual Science